Catena 122 (2014) 61–71

Contents lists available at ScienceDirect

Catena

journal homepage: www.elsevier.com/locate/catena

Modeling wind erosion flux and its seasonality from a cultivated sahelian surface: A case study in Niger

C. Pierre [a,*], G. Bergametti [b], B. Marticorena [b], A. AbdourhamaneTouré [c], J.-L. Rajot [d], L. Kergoat [a]

[a] Geosciences Environnement Toulouse, Université de Toulouse/CNRS/IRD, 14 Avenue Edouard Belin, 31400 Toulouse, France
[b] Laboratoire Interuniversitaire des Systèmes Atmosphériques, LISA, 61 Avenue du Général de Gaulle, 94010 Créteil Cedex, France
[c] Université Abdou Moumouni, Jeune Equipe Associée à l'IRD, Anthropisation et dynamique Eolienne (JEAI ADE), Département de Géologie, BP 10662 Niamey, Niger
[d] IRD Bioemco, UMR IRD/UPMC/CNRS/ENS/UPEC/AgroParisTech, 32 Avenue Henri Varagnat, F-93143 Bondy, France

ARTICLE INFO

Article history:
Received 21 December 2013
Received in revised form 5 May 2014
Accepted 4 June 2014
Available online xxxx

Keywords:
Wind erosion
Sahel
Cropped surfaces
Horizontal flux
Drag partition
Aerodynamic surface roughness

ABSTRACT

Wind erosion can strongly affect the cultivated areas in semi-arid regions, through soil losses and/or decrease in nutrient contents. Additionally, dust emitted by aeolian erosion affects both the biogeochemical cycles and the Earth radiation budget. Modeling wind erosion and dust emission remains complex especially in semi-arid regions where vegetation interacts with the wind field and may act as a protection of the soil. An existing and widely used wind erosion model is tested in the present study to check the capacity to reproduce observations collected over a millet field and a neighboring bare plot in southwestern Niger during a three-year period. Observations of sediment horizontal fluxes and of vegetation growth and decay show that most of the eroded mass is due to major events occurring at the end of the dry season and at the beginning of the rainy season for the millet field, while erosion also occurs during the dry season for the bare soil plot. Horizontal erosion fluxes were computed with and without obstacles and compared to the measurements. Simulations were found in a good agreement with erosion measurements for both bare and millet plots, in terms of temporal dynamics, reproduction of the major events and annual quantities.

Accumulated horizontal fluxes over the millet plot were found to be much lower than over the bare plot for both observations and simulations (respectively 235 to 565 kg m^{-1} y^{-1} and 332 to 526 kg m^{-1} y^{-1} over the millet plot; and 773 to 2692 kg m^{-1} y^{-1} and 1003 to 1986 kg m^{-1} y^{-1} for the bare plot). Total values over the 3-year period also show a much stronger (by a factor 3 to 4) wind erosion on the bare plot (5365 kg m^{-1} y^{-1} for observations, 4548 kg m^{-1} y^{-1} for simulations) than on the cropped one (1357 kg m^{-1} y^{-1} for observations, 1398 kg m^{-1} y^{-1} for simulations). Modeling is therefore able to represent anthropogenic impacts on wind erosion over typical Sahelian surfaces.

1. Introduction

In semi-arid areas, the soils support crop production for local population and/or fodder production for livestock. Yet, they can undergo huge mass losses due to wind erosion (see Bielders et al., 2004 for a review). Wind erosion decreases nutrient content (Okin et al., 2006) since nutrients are generally concentrated in the surface layer of the cultivated soils (Bielders et al., 2002). Annual nutrient losses can reach quantities of the same order of magnitude than those consumed for annual millet production (Sterk and Stein, 1997). Most of the eroded sediment redeposit close to the erosion area; for instance in fallows (Bielders et al., 2004) or even in specific areas within a cropped field, creating islands of fertility (Wezel et al., 2000). However, the finest part of these sediments can be transported over long distances. When deposited, these mineral particles play a decisive role on the availability of some nutrients such as iron or phosphorus for large oceanic and continental regions (e.g. Jickells et al., 2005; Swap et al., 1992). During their atmospheric transport, these particles contribute on average to 20% of the total aerosol optical thickness. Consequently, they affect the radiation balance of the Earth and thus its climate (e.g. Tegen et al., 1997).

Over the last years, significant progresses have been made in the understanding and modeling of wind erosion processes. In particular, specific models based on original and explicit process parameterizations have been developed (Gillette and Passi, 1988; Marticorena and Bergametti, 1995; Shao et al., 1996). These models helped prioritizing factors controlling wind erosion, such as aerodynamic conditions and soil properties (e.g. Marticorena et al., 1997) or soil moisture (Fécan et al., 1999). However, when the global emissions of mineral aerosols are considered, the respective contributions of bioclimatic changes and human management remain particularly difficult to distinguish.

* Corresponding author.
E-mail addresses: caroline.pierre@get.obs-mip.fr (C. Pierre), gilles.bergametti@lisa.u-pec.fr (G. Bergametti), beatrice.marticorena@lisa.u-pec.fr (B. Marticorena), doudu2000@yahoo.fr (A. AbdourhamaneTouré), jeanlouis.rajot@ird.fr (J.-L. Rajot), laurent.kergoat@get.obs-mip.fr (L. Kergoat).

http://dx.doi.org/10.1016/j.catena.2014.06.006
0341-8162/

30 to 50% of the total atmospheric dust load would be due to climatic changes and human activities according to Tegen and Fung (1995). More recently, Tegen et al. (2004) estimated that dust emitted from the 'land use source' contributes up to 10% to the global dust load against 0% to 50% for Mahowald et al. (2004), who used the same data but different model and methodology. Yoshioka et al. (2005) proposed a contribution of 'new' desert areas and cultivation sources of 0 to 25% based on comparison between simulations and the Absorbing Aerosol Indices (AAIs) derived from Total Ozone Mapping Spectrometer (TOMS) measurements.

Recently, simulations of Sahelian dust emissions combining a Sahelian vegetation model with a dust emission model were performed (Pierre et al., 2012). These simulations aimed at estimating the Sahelian contribution of wind erosion to the atmospheric dust content in the theoretical case of a Sahel without crops and livestock. These simulations imply a very low contribution to dust emissions of such a "non-perturbated" Sahel, in agreement with available observations (Pierre et al., 2012). However, local wind erosion measurements performed in Sahelian cultivated areas are commonly reported (under about 500 mm of precipitation), strongly suggesting that the contribution of cropped areas to local wind erosion and dust emissions should be significant in the present climatic conditions (Abdourhamane Touré et al., 2011; Bielders et al., 2002; Rajot, 2001; Valentin et al., 2004).

Thus, the objective of the present study is to investigate the capacity of wind erosion models to quantitatively simulate the wind erosion over a bare soil and a cropped plot along a seasonal cycle. A 3-year experimental dataset of surface properties and wind erosion is used to discuss the quality of the simulations.

2. Material and methods

2.1. Physical principles

Wind erosion is a power function of the wind speed, but it occurs only when a threshold in wind speed is exceeded (Bagnold, 1941). This threshold is usually expressed in terms of friction velocity, which is proportional to the wind shear stress on the surface. The threshold depends on the top soil layer characteristics and on the presence of non-erodible elements on its surface. These non-erodible elements drive the partition of the energy provided by the wind on the surface (Raupach, 1992). They absorb part of the energy while the rest of it is exerted on the intervening surface, thus modifying the threshold wind friction velocity (Gillette, 1979). The frequency of wind erosion events depends on the number of times the wind speed reaches this threshold and the intensity of wind erosion fluxes depends on the amount by which the threshold is exceeded. Thus the description of the part of the wind energy transmitted to the soil surface is a key parameter to quantify dust emissions accurately.

In order to estimate the wind erosion threshold over rough surfaces, different models of drag partition between obstacles and erodible surfaces have been proposed. These drag partition models describe how the energy provided by the wind splits between the obstacles and the bare soil surface. Generally, the models use as input data either the aerodynamic roughness length of the surface (Marticorena and Bergametti, 1995), or the obstacle drag coefficients and the roughness density (ratio of the sum of obstacle frontal surfaces, face to wind, per unit surface at the soil) (Raupach et al., 1993). These schemes have been shown to be particularly relevant for relatively low roughness density and uniformly distributed obstacles (Darmenova et al., 2009).

In order to extent the *Marticorena and Bergametti's* drag partition scheme to typical desert vegetation types, MacKinnon et al. (2004) adjusted it to in situ measurements performed in Central Mojave Desert, USA. The new expression derived is thus adapted for higher roughness lengths.

The *Raupach*'s model requires several parameters that are difficult to determine in the case of a real field (e.g. β: the ratio of obstacle to surface drag coefficient, and *m*: the spatiotemporal variability of the wind shear stress on the surface around the obstacle). Since the aerodynamic roughness length is an integrative value for a given surface, *Marticorena and Bergametti*'s model will be considered here as more relevant for the present study. Its skills to represent wind erosion from a bare surface and from a cultivated plot will be investigated.

2.2. Parametrizations to be tested

For a given particle diameter D_p for a surface with obstacles, the Marticorena and Bergametti (1995) drag partition expresses the threshold wind friction velocity U_t^* as the ratio of the threshold wind friction velocity of the bare surface U_{ts}^* for the same particle diameter on an efficient fraction f_{eff}:

$$U_t*\left(D_p, Z_0, z_{0s}\right)=U_{ts}*\left(D_p, z_{0s}\right) / f_{eff}(Z_0, z_{0s}) \quad (1)$$

where

$$f_{eff}(Z_0, z_{0s})=1-(ln(Z_0/z_{0s})/ln(\delta/z_{0s})) \quad (2)$$

and, according to Elliot (1958):

$$\delta/z_{0s} = a(X/z_{0s})^p \quad (3)$$

where Z_0 is the aerodynamic roughness length of the surface with the obstacles and z_{0s} the aerodynamic roughness length of the bare soil between obstacles; δ is the height of the Internal Boundary Layer (IBL) that is assumed to develop between the roughness elements, and X is related to the distance downstream of a given obstacle.

Marticorena and Bergametti (1995) validated expression *(1)* by comparison to portable wind-tunnel measurements on various non-vegetated erodible sites of the United States (Gillette et al., 1982; Nickling and Gillies, 1989).

In expression *(3)*, p can be taken equal to 0.8 according to Elliot (1958) and Marticorena and Bergametti (1995). These last authors also determined a mean value of δ by computing the efficient fraction for various size and density of obstacles. They also concluded that a constant value of $X = 10$ cm and $a = 0.7$ (following the corrected version of this parameterization, as in Darmenova et al., 2009) gave satisfying agreement with Marshall's (1971) measurements. Finally:

$$f_{eff}=1-\left(\left(ln(Z_0/z_{0s})/ln\left(0{,}7*(10cm/z_{0s})^{0.8}\right)\right)\right. \quad (4)$$

with Z_0 and z_{0s} in cm.

As mentioned above, MacKinnon et al. (2004) proposed an adaptation of this parameterization to extend its use to rougher vegetated surfaces. This study is based on measurements from vegetated sites in the Mojave Desert (USA), where porous vegetation can be dense without preventing the wind shear stress to reach the surface (Wolfe, 1993). Whereas the largest value of the aerodynamic surface roughness considered by Marticorena and Bergametti (1995) and Marticorena et al. (1997) was about 0.2 cm, values reported by Wolfe (1993) reach 3.8 cm and even 7 cm for one of the 11 study sites of MacKinnon et al. (2004). These authors have adjusted the drag partition scheme by choosing a lower and an upper bound of threshold friction velocities encompassing both *McKinnon*'s and *Marticorena et al.* values. These bounds correspond respectively to a smooth surface of the most erodible particle size (60 to 120 μm in diameter, $U_t^* = 21.7$ cm s^{-1}), and to a threshold friction velocity of 100 cm s^{-1} for an aerodynamic surface roughness of 10 cm. They finally obtained a value of 12,255 cm for parameter X:

$$f_{eff}=1-\left(ln(Z_0/z_{0s})/\ ln\left(0{,}7*(12255\ cm/z_{0s})^{0.8}\right)\right. \quad (4')$$

The *McKinnon*'s parameterization has already been used by Darmenova et al. (2009) to simulate dust emissions from the semi-arid regions of Central and Eastern Asia, yielding to satisfying results.

2.3. Dataset

2.3.1. Description of the experiment

Millet crop is the dominant crop in cultivated Sahel (ICRISAT/FAO, 1996) and therefore it provides a representative case for wind erosion. In order to check the capacity of *Marticorena and Bergametti's* drag partition scheme to reproduce wind erosion fluxes over a millet crop, the results of this model have to be compared to ground observations on a Sahelian site. To do so, the dataset described in Abdourhamane Touré et al. (2011) will be used. Indeed, these authors performed measurements of horizontal flux, wind speed and rainfall with a good temporal coverage from March 2006 to the end of 2008. In this area, about 60 km east of Niamey, most soils are particularly sandy, except for some outcrops and iron pans on the plateaus and some depressions and river beds, which are minority. Cultivation has strongly expanded, particularly during the last decades, and pastoral activities are also important (Hiernaux et al., 2009).

Two plots (100 m × 150 m each) were instrumented near Banizoumbou (13.54°N, 2.66°E) by Abdourhamane Touré et al. (2011). One of the monitored plots was cropped with millet in a traditional way (Picture 1), while the other one was regularly kept as a bare surface by suppression of any vegetation. These plots are extremely sandy and do not exhibit any gravel or clod. The details on the instruments and monitoring are given in Abdourhamane Touré et al. (2011). Briefly, a mast equipped with 4 anemometers at 0.35 m, 0.70 m, 1.40 m and 2.50 m above soil level was implanted in the middle of each of the two plots, and wind direction and rainfall were measured in a dust monitoring station 200 m away (Marticorena et al., 2010). The annual temporal coverage of the wind measurements is usually greater than 70% (monitoring started in March 2006 and ended at the beginning of September 2008): values are missing from August 2006 to the end of the year for the bare plot, and in February 2007 for the cropped plot. Millet height during the rainy season, crop residue cover and density after harvest were also monitored over the cropped plot.

On each plot, 25 poles of 3 Big Spring Number Eight (BSNE; Fryrear, 1986) sand traps at 5, 15 and 35 cm heights measured the horizontal flux G, which is constituted by the soil grains following a horizontal movement (called saltation) through ballistic trajectories. The horizontal flux G is then computed by vertical integration of the flux density from the different sand traps of a pole. Most of the annual erosion flux results from a few major events: the cumulative contribution of the 10 strongest annual events is greater than 90% of the annual value for each monitored year. Threshold friction velocities were deduced from acoustic sensor measurements (one Saltiphone for each plot, Spaan and van den Abeele, 1991) registering particle impacts accumulated over 5 min. Because of technical difficulties (sensors not being sensitive to very small grains at low wind speed), the threshold is assumed to be reached when the probability of erosion, computed as the frequency of recorded grain impacts for a given interval of wind speed, is 50%. This value is computed over one-month periods to improve the confidence level.

Consequently, the main limitations of these measurements are due to different factors, like the occasional lack of wind measurements, usually due to power shortage of the monitoring instruments. It is also difficult to determine the exact periods of occurrence of the horizontal fluxes measured with the sand traps from the date of these specific measurements (which depend on the timing of sediment collection) and from acoustic sensor measurements. Integration over time is therefore recommended. However, the dataset present the great advantage of providing values simultaneously for both a smooth surface and the corresponding vegetated one for the same soil type and climatic conditions, in terms of surface roughness, vegetation characteristics and wind erosion: thus it is very useful for testing models. The parameterizations presented above will be tested first in the case of the bare plot to check the consistency of the model in this simple case, before adding the effect of the drag partition.

2.3.2. Obtained measurements

Fig. 1 provides an example of these measurements for year 2006. Note that, as expected, the horizontal flux is always greater for the bare plot than for the cropped one, confirming the sheltering effect of the green vegetation and its residue (Abdourhamane Touré et al., 2011). Most of the wind erosion occurs during the end of the dry season and the beginning of the rainy season (between Days of Year – DoY – 150 and 200, i.e. between around May 30th and July 20th), corresponding to the beginning of millet growth. Additionally, the authors

Picture 1. Millet field (plot PB) in Niger (Banizoumbou, 13.54°N, 2.66°E), in 2006, August 8th.

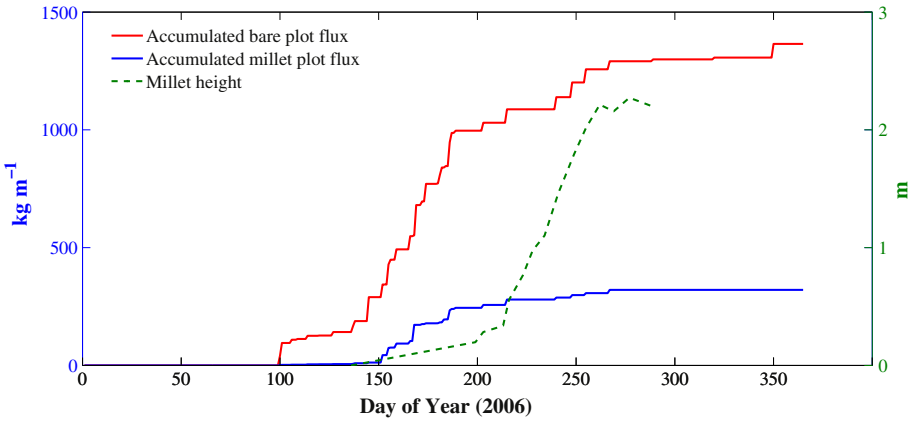

Fig. 1. Measured millet height for the cropped plot PB (right vertical scale) and accumulated horizontal flux (left vertical scale) for the bare and cropped plots over the year 2006 (data from Abdourhamane Touré et al., 2011).

observed that wind erosion becomes weaker around DoY 200 over both plots. This shows that the decrease in strong wind frequency and duration plays a major role in the decrease of wind erosion, which is enhanced by the growth of the millet vegetation cover in the case of the cropped plot (Abdourhamane Touré et al., 2011). Thus the beginning of the millet growth is the period during which the drag partition must be precisely assessed.

Aerodynamic roughness Z_0 can be estimated from the wind profiles as measured by the anemometers, by fitting the logarithmic law of the wind profile (Priesley, 1959):

$$U(z) = (U*/k)x\ ln(z/Z_0) \quad (5)$$

with k being the Von Karman constant ($k = 0.4$), z the height of measurement of wind speed $U(z)$ and U^* the friction velocity. A daily Z_0 has been be computed as the daily median of the values estimated from the 5 minute-average of 10 second-wind measurements (Abdourhamane Touré et al., 2011). In the absence of temperature profile, the calculation of Z_0 has been made by assuming thermal dynamic neutrality: when winds are strong enough, the temperature effect is considered as negligible (e.g. Lancaster and Baas, 1998). More precisely, Z_0 values are retained only when wind speed at 0.35 m is greater than 2.5 ms^{-1}. Finally, the Z_0 values mentioned below are daily medians of these results: indeed, a daily time-step is relevant to represent the temporal variability of the surface properties.

The daily aerodynamic roughness lengths Z_0 are plotted for the measurement period on Fig. 2. The Z_0 of the bare plot remains lower than the Z_0 on the cultivated one and it does not show any tendency because there are not important changes of its surface during these years. Oppositely, Z_0 on the cultivated plot tends to decrease from the clearing of the field (around January) down to the beginning of the crop growth. Thus, the lowest values of Z_0 are generally observed during the very beginning of the rainy season when crop residues have partly disappeared and when the millet growth has not started yet. Abdourhamane Touré et al. (2011) mentioned a 1-month time-shift between the first rainfall allowing sowing and millet growth. Harvest takes place in October. After harvest, millet straws are left standing on the plot, and they are laid down around the beginning of January for clearing. This typical cycle of Z_0 can vary from a year to another according to the field productivity (mainly driven by the rainfall distribution), the farming practices, the rainfall regime, and the intensity of livestock grazing.

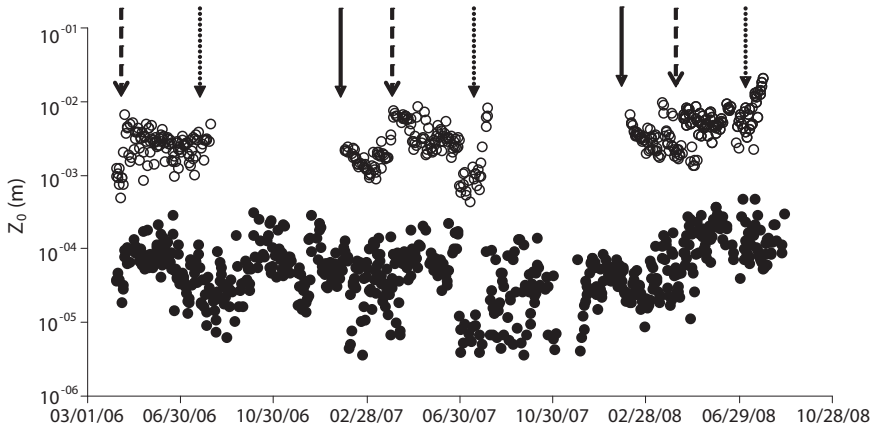

Fig. 2. Aerodynamic roughness length Z_0 on the bare plot (full circles) and on the cropped one (open circles). Dashed arrows indicate the change in wind direction between the easterly Harmattan dry wind and the south-westerly monsoon humid wind. Solid arrows indicate the clearing of the cropped plot and dotted arrows indicate the beginning of Z_0 increase due to crop growth. Note that on the cropped plot, aerodynamic roughness length was only assessed until millet attained a height of 0.7 m. Figure redrawn from Abdourhamane Touré et al. (2011).

3. Results and discussion

3.1. Model application

A high temporal and spatial variability being inherent to measurements of aerodynamic surface roughness, we attempted to derive the most relevant values of this variable for the cropped plot. Contrarily to the bare plot, the Z_0 value changes significantly with times in that case, and it displays a strong seasonality (Abdourhamane Touré et al., 2011).Yet, a compromise must be made in order to get a good confidence in the Z_0 value and to reproduce its dynamics. In terms of spatial variability and heterogeneity, the present methodology aimed at selecting the Z_0 value representing the entire plot, which size was of about 1 ha. Therefore, Z_0 values were selected depending on the wind direction in order to provide the maximum fetch, i.e. for wind direction corresponding to the diagonals of the plot. In terms of temporal variability, daily values allow characterizing the dynamics of the surface properties while minimizing the dispersion of the measured values. Additionally, the roughness length value is retained only before millet height reaches 0.7 m. Indeed at that point the height of the vegetation reaches the height of the instruments, preventing an accurate computation of the wind logarithmic profile.

The *Marticorena and Bergametti's* scheme requires parameters for Eqs. (1) and (4) that have been derived from field observations and compared to existing literature values for similar case studies. Particularly, the drag partition scheme requires value of z_{0s} and $U_{ts}{}^*$ to be applied to the cropped plot. For that purpose, measurements over the bare plot are used, assuming that the soil characteristics are the same than for the bare part of the cropped one. This assumption is reasonable since the two plots, separated by a vegetated stripe 20 m wide, were chosen within the same original field. Moreover, the erosion fluxes measured during one year (2005) on the two plots, before treatment of the bare plot in 2006, were found to be identical (Abdourhamane Touré et al., 2011). The median of the daily values of roughness length over the bare plot for the 2006–2008 period is:

$$z_{0smes} = 5.5\ .10^{-5} m \left(+/-4.2\ .10^{-5} m\right)$$

The standard deviation is relatively high (almost equal to the median z_{0s}). This illustrates the difficulty of inferring such values from field measurements. Alternative methods to estimate z_{0s} can be used to compare to this measured value. In the case of a static granular bed composed of grains of the same diameter D, various estimates of the smooth aerodynamic roughness length have been proposed: $z_{0s} = D/30$ in Nikuradse (1933) and Bagnold (1941), $z_{0s} = D/24$ in Schlichting and Gersten (2000) and $z_{0s} = D/10$ in Kamphuis (1974) and Andreotti et al. (2006). For natural surfaces, where various grain sizes are simultaneously present in the soil, Marticorena and Bergametti (1995) and Laurent et al. (2006) proposed to derive the smooth aerodynamic roughness length z_{0s} from the median diameter (in terms of mass) of the coarsest population of undisturbed soil particles $D_{p\ coarse}$:

$$z_{0sssd} = D_{p\ coarse}/30 \tag{6}$$

However, the classical sedimentology-based roughness relation:

$$z_{0sssd} = 2\ D_{p\ \ coarse}/30 \tag{6'}$$

is generally considered as a better approximation for natural surfaces (see for example Farrel and Sherman, 2006).

For our site, the grain-soil size distribution can be represented, following Chatenet et al. (1996), by a combination of 3 lognormal distributions whose characteristics are given in Table 1 (Sabre, 1997).

Thus, the diameter of the coarsest population being 650 μm:

$z_{0sssd} = 2.2 \times 10^{-5}$ m according to Eq. (6) and $z_{0s\ ssd} = 4.3 \times 10^{-5}$ m according to Eq. (6')

These values are in good agreement with the median of the daily values estimated from the field measurements (5.5×10^{-5} m +/− 4.2×10^{-5} m). This result is noticeable given the accuracy and the difficulty of such field observations. It also confirms that the bare plot has a very smooth surface, without any gravels and clods. Considering the limitations of such measurements, two values will be used as boundary values for z_{0s}: the measured one (5.5×10^{-5} m) and the measured one plus a standard deviation (9.7×10^{-5} m). The corresponding results will be considered to illustrate the uncertainty. The measured value of z_{0s} minus a standard deviation yields to unrealistically low surface roughness and modeled wind erosion, and the corresponding results will not be presented below.

Following a similar methodology than for the smooth aerodynamic surface roughness z_{0s}, the threshold friction velocity for the smooth surface $U_{ts}{}^*$ is deduced from the measurements performed by Abdourhamane Touré et al. (2011) for the bare plot, i.e.:

$$U_{ts}* = 0.22\ m.s^{-1}$$

This value is very close to the minimum threshold wind friction velocity obtained in wind tunnel for loose soil particles having a diameter close to 100–200 μm (e.g. Chepil, 1945).

Table 1
The three log-normal populations of the undisturbed soil grain size distribution of the bare plot.

	Population 1	Population 2	Population 3
Mass fraction (%)	8.4	80.1	11.5
Mass median diameter (μm)	76	249	650
Standard deviation	1.20	1.58	1.26

To represent the contributions of each soil grain size population to the horizontal flux of sediment, the expression proposed by Marticorena and Bergametti(1995) is used:

$$U_t^*\left(D_p\right)=\begin{cases}0.129\dfrac{\left(\dfrac{\rho_p g D_p}{\rho_a}\right)\left(1+\dfrac{0.006}{\rho_p g {D_p}^{2.5}}\right)^{0.5}}{\left(1.928\left(a_1 {D_p}^{a_2}+a_3\right)^{0.092}-1\right)^{0.5}} & \text{if } 0.03<R<10\\ 0.12\left(\dfrac{\rho_p g D_p}{\rho_a}\right)^{0.5}\left(1+\dfrac{0.006}{\rho_p g {D_p}^{2.5}}\right)^{0.5}\left[1-0.0858\exp\left(-0.0617\left(\left(a_1 {D_p}^{a_2}+a_3\right)-10\right)\right)\right] & \text{if } R>10\end{cases} \quad (7)$$

where ρ_p is the particle density (2.65 g/cm^3), ρ_a the air density (0.001227 g/cm^3), 0.006 is in g cm$^{0.5}$ s^2, $a_1 = 1331$, $a_2 = 0.38$, $a_3 = 1.56$, g is the gravity and R the Reynolds number (computed as a function of the particle diameter). Once the threshold friction velocity is known, the horizontal flux can be estimated following White (1979), integrated on the grain-size distribution according to the relative surface of each grain size population S_{rel}:

$$G = E\ c\left(\rho_p/g\right)U^{*3}\sum_{Dp}\left(1+U_t^*\left(D_p,Z_0,z_{0s}\right)/U^*\right)\left(1-U_t^*\left(D_p,Z_0,z_{0s}\right)^2/U^{*2}\right)dS_{rel}\left(D_p\right)dD_p \quad (8)$$

where E is the erodible surface ratio (i.e. not covered by obstacles). More details can be found in Marticorena and Bergametti (1995).

The erodible surface ratio is equal to 1 in the case of the bare plot, but it depends on the millet cover for the crop plot. A description of the vegetation cover at the beginning of the year has been taken from Fig. 7 in Abdourhamane Touré et al. (2011) by setting the clearing of the field on January 1st. For the millet growth period, preexisting parameterizations of a Sahelian vegetation model (STEP: Sahelian Transpiration Evaporation and Productivity model; Mougin et al., 1995; Hiernaux et al., 2009) have been used to estimate millet biomass and then surface cover from the measurements of millet height. The resulting values of the erodible surface ratio are illustrated in Fig. 3 for year 2007.

As observed by Bielders et al. (2004) for several Sahelian study sites, surface cover by crop residues decreases (from 12% at January 1st) during the beginning of the year because of the disappearing of the residues: thus the erodible surface ratio increases and reaches almost 1, at the beginning of the rainy season just before green millet grows. Then, millet pockets cover an increasing part of the surface until reaching a maximum (when about 1/3 of the surface is covered) at the end of July. Once the cover fraction of millet is maximal, it is supposed to remain approximately constant until harvest. The corresponding estimation of the erodible surface ratio (during the late rainy season and the dry season before field clearance) is idealized (dot line on Fig. 3), since most of the annual wind erosion has occurred earlier (typically in May and June).

The effects of soil moisture on threshold wind friction velocities and on the saltation fluxes have also to be taken into account. Since no soil moisture measurements are available for the study site, we considered that wind erosion is nil during a rain event and the following 24 h, which is appropriate for convective rainfall in the usually hot and sunny Sahelian climate. Moreover, the short time-step of the rainfall data permits to represent erosion events driven by the gust fronts that often precede the convective rain.

For comparison between simulated and measured horizontal flux, the mean of the 10 strongest values of the sands traps are used for each erosion event. Indeed, the 10 strongest values are supposed to better correspond to a stable erosion flux, which will not be captured by the sand traps located near the border of the plot. The mean of all 25 sand traps values (as in Abdourhamane Touré et al., 2011) will also be indicated as representative value of wind erosion over the entire plots. In addition, for consistency reasons, measured fluxes are assumed to be nil if they correspond to missing data in the wind measurements.

Besides, in the case of the millet plot, fluxes are also assumed to be nil as soon as the millet is 0.7 m high (around mid-August in 2006 and 2007, around July 20th in 2008) since no reliable aerodynamic surface roughness can be computed from this date. Measured wind erosion from these dates to the end of the corresponding year is of about 5% of the annual value.

3.2. Wind erosion modeling: case of bare plot

Horizontal fluxes have been computed for the bare plot for the years 2006 to 2008 with friction velocities U^* computed every 5 min (i.e. the time step of wind measurements) from the wind measured at 2.5 m high by using a logarithmic profile (Eq. (5)) and the measured aerodynamic surface

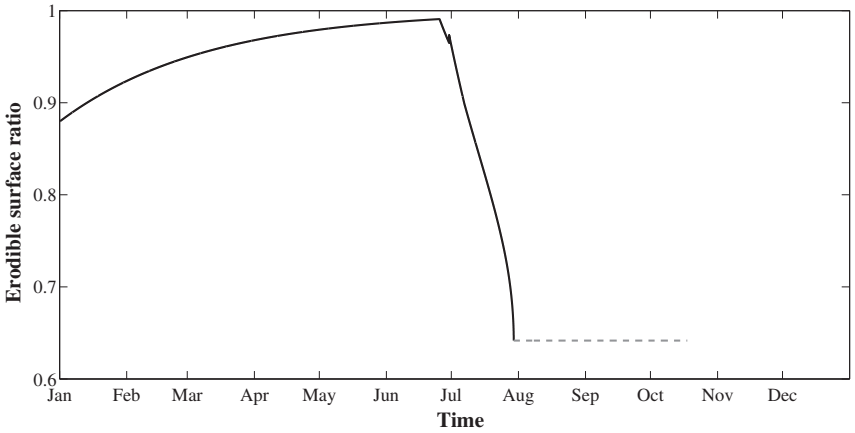

Fig. 3. Erodible surface ratio in year 2007 for the cropped plot.

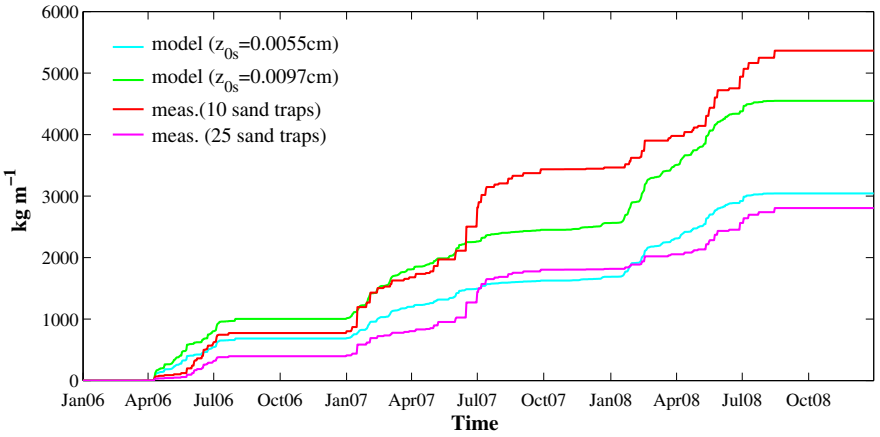

Fig. 4. 2006 to 2008 accumulated horizontal daily flux, simulated ($z_{0s} = 5.5 \times 10^{-5}$ m and $z_{0s} = 9.7 \times 10^{-5}$ m) and measured (mean of 25 and 10 sand traps) for the bare plot.

roughness z_{0s} (see **3.1**). The consistency of these U^* values with values obtained from wind speed measured at 1.40 m and 0.70 m has been checked: no significant bias is induced by the absence of the thermal profile correction. The threshold friction velocity is computed from Eq. (7).The horizontal sediment flux G (expressed in kg m^{-1}) is computed from Eq. (8) every 5-min to take advantage of the high resolution of wind measurements, and summed over a daily time step to be compared to horizontal flux measurements (Fig. 4). Annual and pluriannual cumulated values are also computed and compared to field observations (Table 2).

Simulated horizontal fluxes computed by using the measured surface roughness ($z_{0s} = 5.5 \times 10^{-5}$ m) are of the same order as the mean of all 25 sand trap measurements, but clearly lower than the mean value of the 10 strongest records from the sand traps. Since the wind erosion model is designed to reproduce at stabilized situation, it means that simulations with $z_{0s} = 5.5 \times 10^{-5}$ m underestimates the horizontal flux. Yet, when taking into account the uncertainty on the measured bare surface roughness value ($z_{0s} = 9.7 \times 10^{-5}$ m), the mean value of the 10 strongest records from the sand traps is well reproduced by the model, particularly for year 2008.The difference in simulated horizontal fluxes when using these two different values for the aerodynamic smooth surface roughness indicates that the wind erosion model is highly sensitive to z_{0s}.

The interannual variability and the seasonality are well reproduced: both simulated annual eroded sediment masses are much stronger in 2007 and 2008 than in 2006, and the strongest events, occurring between May and July, are well represented (Fig. 5). Wind erosion is very weak for both measurements and simulations from September 2007 to January 2008. However, the annual horizontal flux is overestimated (underestimated) by the model in year 2006 and 2008 (2007) ($z_{0s} = 9.7 \times 10^{-5}$ m compared to 10 sand traps). Overestimation can be due to the uncertainty in threshold friction velocity and/or in friction velocity (i.e. in wind measurements and/or in the aerodynamic roughness length z_{0s}). Underestimation might be due to the representation of wind erosion inhibition during and after rainfall. Nevertheless, the agreement between simulations and observations is

Table 2
Measured and simulated annual horizontal fluxes (kg m^{-1} y^{-1}) for the bare plot.

	Annual simulated flux $z_{0s} = 5.5 \times 10^{-5}$ m	Annual simulated flux $z_{0s} = 9.7 \times 10^{-5}$ m	Annual measured flux 10 strongest samplers	Annual measured flux All measurements (25 samplers) (Abdourhamane Touré et al., 2011)
2006	685	1003	773	396
2007	1004	1559	2692	1420
2008	1355	1986	1900	988
Total	3044	4548	5365	2804

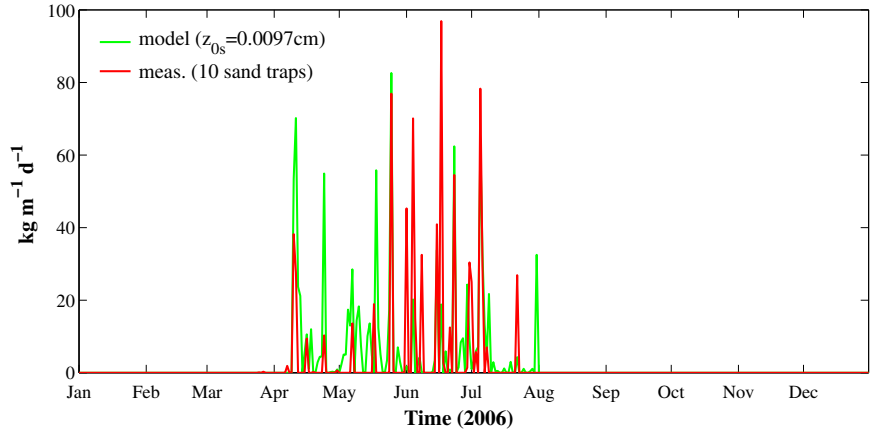

Fig. 5. Simulated ($z_{0s} = 9.7 \times 10^{-5}$ m) and measured (mean of 10 sand traps) horizontal dust fluxes for the bare plot for year 2006.

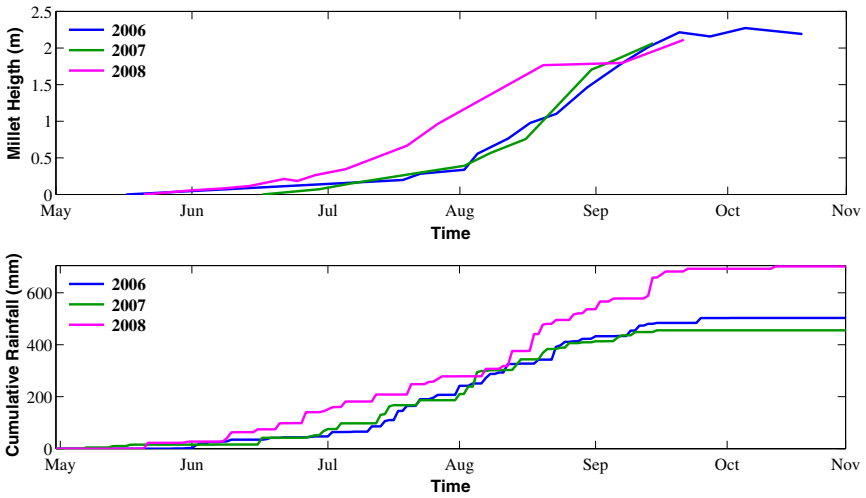

Fig. 6. Millet height (m) (top) and cumulative rainfall (mm) (bottom) for the millet plot in 2006, 2007 and 2008.

satisfying over the 3-year period considered. Given the uncertainty on the daily flux measurements, correlation coefficients are computed for horizontal fluxes cumulated over periods of 15 and 30 days. These correlation coefficients are respectively 0.58 and 0.64 for $z_{0s} = 9.7 \times 10^{-5}$ m and 10 sand traps, and 0.53 and 0.59 for $z_{0s} = 5.5 \times 10^{-5}$ m and all 25 sand traps. The value of $z_{0s} = 9.7 \times 10^{-5}$ m will be retained for the case of the cropped plot as a satisfying estimates regarding these results. $z_{0s} = 5.5 \times 10^{-5}$ m is also retained to illustrate uncertainty.

3.3. Wind erosion modeling: case of the cropped plot

As for the bare plot, friction velocity U^* has been computed every 5-min following Eq. (5). The erodible surface ratio E varies as described in Section 3.1. The horizontal flux is computed with a 5-min time-step and summed every day for comparison to measurements.

McKinnon's parameterization for the efficient fraction (Eq. (4')) yields to simulated horizontal fluxes which are much higher than the measured ones (not shown). This is likely related to the values of Z_0 considered here: typically about 0.5 cm in May and June (when the strongest winds occur and when most of the annual wind erosion is observed) while the MacKinnon et al. (2004) formulation has been designed for much stronger Z_0 values (up to 7 cm). Thus, the *Marticorena and Bergametti* parameterization could be more relevant in the present case study. The discrepancy between measured fluxes and modeled fluxes using the *McKinnon*'s parameterization also raises the question of the importance of the vegetation structure and distribution. Indeed, while *McKinnon's* adaptation has been designed specifically for vegetated surfaces, the measurements used to derive this parameterization have been performed over types of surfaces and vegetation too different than those corresponding to the present study to be adapted here. More precisely, MacKinnon et al. (2004) worked with measures obtained over surfaces mainly vegetated by bushes. It can be assumed that these bushes have structural properties that differ significantly from those of young millet pockets, for example in terms of geometry, flexibility and porosity, as well as spatial distribution.

The rainy season was earlier and more regular in 2008 (702 mm) than in 2006 (503 mm) and 2007 (456 mm), with the first rains occurring at the end of May instead of the end of June and without any dry spell afterwards. Consequently, millet growth started about 1 month earlier in 2008 than in 2006 and 2007 (Fig. 6). Thus, vegetation cover and the corresponding aerodynamic roughness length around May and June are significantly larger in 2008 than for the 2 previous years (Fig. 2).

As mentioned by MacKinnon et al. (2004), the X parameter in the expression of the drag partition is related to the roughness element properties. This X parameter might be considered dependent on the dimensions of the roughness elements. Gravels and pebbles in the case of Marticorena and Bergametti (1995) yielded to $X = 10$ cm, while vegetation such as bushes for MacKinnon et al. (2004) lead to $X = 12{,}255$ cm. In the present case, millet has not grown much during the most erosive period of years 2006 and 2007, but it constitutes larger obstacles at the same period in 2008. Therefore Eq. (4) has to be adapted to take into account the different roughness properties on the cropped plot for year 2008, while the *Marticorena and Bergametti's* parameterization describes well years 2006 and 2007.

Following the methodology proposed by MacKinnon et al. (2004), the adaptation proposed here is based on varying the value of the X parameter. Erosion fluxes for parameter X varying from 10 cm (*Marticorena and Bergametti's* value) to 12,255 cm (*McKinnon's* value) were computed for the year 2008: values of X close to 40 cm provide both acceptable annual sums and occurrence of the major events. Thus for year 2008, Eq. (4) becomes:

$$f_{eff} = 1\text{-}\left(ln(Z_0/z_{0s})/ln\left(0{,}7*(40cm/z_{0s})^{0.8}\right)\right) \tag{9}$$

Table 3
Measured and simulated annual horizontal fluxes (kg m^{-1} y^{-1}) for the cropped plot.

	Annual simulated flux $z_{0s} = 5.5 \times 10^{-5}$ m	Annual simulated flux $z_{0s} = 9.7 \times 10^{-5}$ m	Annual measured flux 10 strongest samplers	Annual measured flux All measurements (25 samplers) (Abdourhamane Touré et al., 2011)
2006	182	332	235	137
2007	346	540	557	307
2008	279	526	565	320
Total	807	1398	1357	764

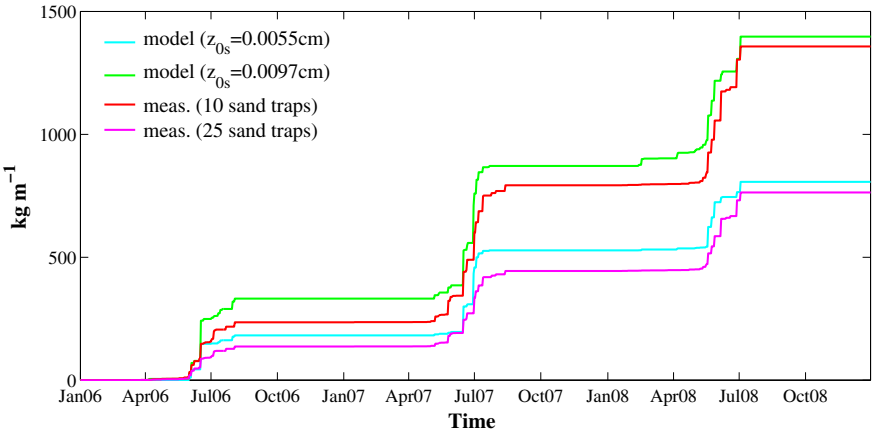

Fig. 7. 2006 to 2008 simulated ($z_{0s} = 5.5 \times 10^{-5}$ m and $z_{0s} = 9.7 \times 10^{-5}$ m) and measured (mean of 25 and 10 sand traps) horizontal dust fluxes for the cropped plot accumulated through time.

Eqs. (1) and (9) yield to threshold friction velocities decreasing during the end of the dry season, from April (respectively 74, 90 and 56 cm s^{-1} for years 2006, 2007 and 2008 with $z_{0s} = 9.7 \times 10^{-5}$ m) to June or July (resp. 60 and 47 cm s^{-1} for years 2006 and 2007). Yet, the threshold friction velocity increases from June onwards for year 2008, because of the early beginning of millet growth. These threshold values are larger than the ones obtained by Abdourhamane Touré et al. (2011) (46 to 36 cm s^{-1}) which corresponded to a 50% erosion probability over one month. However, the present values show the same trend (decrease during the end of the dry season due to the disappearance of crop residues) and they are consistent with wind measurements at 5-minute time resolution since erosion events are well represented by the model (see below, e.g. Fig. 8).The discrepancy between modeled and measured threshold wind friction velocities might be due to the uncertainty on Z_0, related to the assumptions of thermal dynamic neutrality, and to the uncertainty on the measured U_t^*, mainly related to the sensitivity of the acoustic sensors. It can also be due to the heterogeneity of the cropped plot (presence of weeds, distribution of millet pockets and millet stalks) that might have influenced measurements of the acoustic sensor that was positioned in the middle of the plot (while the model attributes a unique threshold to the entire field).

The comparisons between simulations and observations, as in the case of the bare plot, involve simulated results obtained by using the measured values for the smooth roughness length ($z_{0s} = 5.5 \times 10^{-5}$ m) and this value increased by a standard deviation ($z_{0s} = 9.7 \times 10^{-5}$ m). The simulated horizontal fluxes show a good agreement with measurements (Table 3 and Fig. 7). As for the bare plot, agreement is good between simulations and mean of the 10 strongest sand trap measurements per events when using the bare surface roughness plus a standard deviation, while using the median of the aerodynamic surface roughness yield to an underestimation of the horizontal flux by the model. Thus, the model reproduces well the measured stable erosion fluxes for bare surface roughness values z_{0s} which fell in its range of uncertainty.

Total fluxes and interannual variability are also well reproduced, horizontal fluxes being much stronger in 2007 and 2008 than in 2006. The results of our simulations represent the contrasted wind erosion between the bare plot and the cropped one: fluxes in the case of the millet plot (235 to 565 kg m^{-1} y^{-1} for the 10 strongest sand trap measurements, and 332 to 526 kg m^{-1} y^{-1} for simulations with $z_{0s} = 9.7 \times 10^{-5}$ m) are much lower than the fluxes from the bare plot (773 to 2692 kg m^{-1} y^{-1} for the 10 strongest sand trap measurements, and 1003 to 1986 kg m^{-1} y^{-1} for simulations with $z_{0s} = 9.7 \times 10^{-5}$ m)(Table 2). The correlation coefficients are 0.90 when the horizontal fluxes are cumulated over a 15-day period and 0.96 when cumulated over a 30-day period for $z_{0s} = 9.7 \times 10^{-5}$ m and 10 sand traps; they are 0.87 and 0.95 for $z_{0s} = 5.5 \times 10^{-5}$ m and all 25 sand traps.

Total values over the 3-year period represent also the much stronger (by a factor 3 to 4) wind erosion on the bare plot (5365 kg m^{-1} y^{-1} for the 10 strongest sand trap measurements, and 4548 kg m^{-1} y^{-1} for simulations with $z_{0s} = 9.7 \times 10^{-5}$ m) than on the cropped one (1357 kg m^{-1} y^{-1} for the 10 strongest sand trap measurements, and 1398 kg m^{-1} y^{-1} for simulations with $z_{0s} = 9.7 \times 10^{-5}$ m), for both observations and simulations.

Fig. 8 illustrates how the model reproduces the seasonality of horizontal fluxes in the case of year 2007. The strongest events, occurring in May, June and July, are well represented in terms of occurrences as well as intensity.

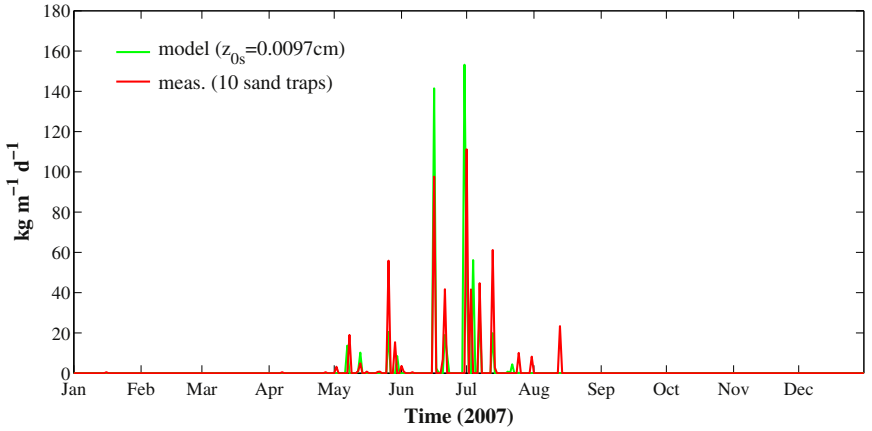

Fig. 8. Simulated ($z_{0s} = 9.7 \times 10^{-5}$ m) and measured (mean of 10 sand traps) horizontal dust fluxes for the cropped plot for year 2007.

4. Conclusion

Three-year (2006 to 2008) measurements of horizontal fluxes of sediment, meteorology parameters and vegetation over a bare plot and a millet plot in Sahelian Niger were used to test the capacity of a wind erosion model to quantitatively reproduce the erosion fluxes. These three years of measurements exhibit a seasonal cycle driven by the alternating dry season, with limited erosion over bare plots only, and monsoon season, with strong erosion caused by a few convection-related gusts during the early rainy season. The observations reveal an interannual variability of the horizontal fluxes and of the vegetation since the rainy season (and thus millet growth) started about one month earlier in 2008 than for the two other years.

The results show that wind erosion can be well reproduced in the case of the bare plot, both in terms of horizontal fluxes, interannual variability and seasonality. A drag partition scheme based on the aerodynamic roughness length was tested over the millet crop. For 2006 and 2007, the drag partition scheme reproduced well the observations, while it required an adaptation inspired by previous work for year 2008 due to higher vegetation at the period during which major events of wind erosion occur. Measured horizontal dust fluxes over the three years were well reproduced by the model for the cropped plot, in terms of amounts, interannual variability and seasonality. Additionally, the contrasted behaviors between the bare and the cropped plots are well captured by the model, which confirms the suitability of this methodology and tools to study these different types of surfaces in terms of wind erosion.

The agreement between observed and measured horizontal fluxes is better for the cropped plot than for the bare one. This is probably due to the fact that the wind friction velocity threshold is low on the bare soil: wind speed is thus frequently close to the erosion threshold, yielding to frequent (but relatively low) errors on horizontal flux estimate. Indeed, the discrepancy between observed and simulated fluxes is mostly caused by small daily values in the case of the bare plot. This is due to the uncertainty on the smooth surface aerodynamic roughness z_{0s} as well as the corresponding wind friction threshold velocity $U_{ts}{}^*$ that are particularly difficult to measure, and thus to simulate. Thus the wind friction velocity U^* which is deduced from the wind speed U and from z_{0s} is also dependent on the accuracy of this parameter derived from field data.

Consequently, challenging issues for modeling wind erosion on cropped Sahelian surfaces concern the estimation of sensitive parameters such as the aerodynamic roughness length of the smooth surface. Besides a good description of the vegetation cover, high temporal resolution rainfall and wind-speed datasets are also required to precisely describe wind erosion and its inhibition due to rain and surface soil moisture over such surfaces, since erosive gusts are sometimes, but not always, rapidly followed by rainfall. Crop field management has to be described also in order to perform regional estimates of the impacts of anthropogenic activities on wind erosion over the Sahel.

Acknowledgments

We would like to thank the Centre National d'Etudes Spatiales (CNES) and the research program CAVIARS (ANR-12-SENV-0007-01) from the French Agence Nationale de Recherche for providing financial support to Caroline Pierre. We thank two anonymous reviewers, who helped to clarify the text. We also thank Eric Mougin for providing up-to-date parameterizations of the STEP model.

References

Abdourhamane Touré, A., Rajot, J.L., Garba, Z., Marticorena, B., Petit, C., Sebag, D., 2011. Impact of very low crop residues cover on wind erosion in the Sahel. Catena 85, 205–214. http://dx.doi.org/10.1016/j.catena.2011.01.002.

Andreotti, B., Claudin, P., Pouliquen, O., 2006. Aeolian sand ripples: experimental evidence of coarsening and saturation. Phys. Rev. Lett. 96, 028001.

Bagnold, R.A., 1941. *The physics of blown sand and desert dunes*, 265 pp. Methuen, New York (265 pp.).

Bielders, C.L., Rajot, J.L., Amadou, M., 2002. Transport of soil and nutrients by wind in bush fallow land and traditionally managed cultivated fields in the Sahel. Geoderma 109, 19–39.

Bielders, C.L., Rajot, J.-L., Michels, K., 2004. L'érosion éolienne dans le Sahel Nigérien: influence des pratiques culturales actuelles et méthodes de lutte. Sécheresse 15 (1), 19–32.

Chatenet, B., Marticorena, B., Gomes, L., Bergametti, G., 1996. Assessing the microped size distributions of desert soils erodible by wind. Sedimentology 43901–43911. http://dx.doi.org/10.1111/j.1365-3091.1996.tb01509.x.

Chepil, W.S., 1945. Dynamics of wind erosion. Soil Sci. 60, 305–320 (397-411, 475-480).

Darmenova, K., Sokolik, I.N., Shao, Y., Marticorena, B., Bergametti, G., 2009. Development of a physically based dust emission module within the Weather Research and Forecasting (WRF) model: assessment of dust emission parameterizations and input parameters for source regions in Central and East Asia. J. Geophys. Res. 114, D14201. http://dx.doi.org/10.1029/2008JD011236.

Elliot, W.P., 1958. The growth of the atmospheric internal boundary layer. EOS Trans. AGU 39, 1048–1054.

Farrel, E.J., Sherman, D.J., 2006. Process-scaling issues for Aeolian transport modeling in field and wind tunnel experiments: roughness length and mass flux distributions. J. Coast. Res. SI39, 384–389.

Fécan, F., Marticorena, B., Bergametti, G., 1999. Parameterization of the increase of the aeolian erosion threshold wind friction velocity due to soil moisture for semiarid areas. Ann. Geophys. 17, 149–157.

Fryrear, D.W., 1986. A field dust sampler. J. Soil Water Conserv. 41, 117–120.

Gillette, D.A., 1979. Environmental factors affecting dust emission by wind erosion. In: Morales, C. (Ed.), Saharan Dust. John Winley, New York, pp. 71–94.

Gillette, D.A., Passi, R., 1988. Modeling dust emission caused by wind erosion. J. Geophys. Res. 93, 14233–14242.

Gillette, D.A., Adams, J., Muhs, D.R., Khil, R., 1982. Threshold friction velocities and rupture moduli for crusted desert soils for the input of soil particles into the air. J. Geophys. Res. 87, 9003–9015.

Hiernaux, P., Ayantunde, A., Kalilou, A., Mougin, E., Gérard, B., Baup, F., Grippa, M., Djaby, B., 2009. Trends in productivity of crops, fallow and rangelands in Southwest Niger: impact of landuse, management and variable rainfall. J. Hydrol. 375, 65–77.

ICRISAT, FAO, 1996. The world sorghum and millet economies: facts, trends and outlook, Patancheru, India. International Crops Research Institute for the Semi-Arid Tropics, and Rome, Italy: Food and Agricultural Organization of the United Nations p. 68.

Jickells, T.D., et al., 2005. Global iron connections between desert dust, ocean biogeochemistry, and climate. Science 38 (5718), 67–71. http://dx.doi.org/10.1126/science.1105959.

Kamphuis, J.W., 1974. Determination of sand roughness for fixed beds. J. Hydraul. Res. 12, 193–207.

Lancaster, N., Baas, A., 1998. Influence of vegetation cover on sand transport by wind: field studies at Owens Lake, California. Earth Surf. Process. Landf. 23, 69–82.

Laurent, B., Marticorena, B., Bergametti, G., Mei, F., 2006. Modeling mineral dust emissions from Chinese and Mongolian deserts. Global Planet. Chang. 52, 121–141. http://dx.doi.org/10.1016/j.gloplacha.2006.02.012.

MacKinnon, D.J., Clow, G.D., Tigges, R.K., Reynolds, R.L., Chavez Jr., P.S., 2004. Comparison of aerodynamically and model-derived roughness lengths (z_o) over diverse surfaces, central Mojave Desert, California, USA. Geomorphology 63, 103–113. http://dx.doi.org/10.1016/j.geomorph.2004.03.009.

Mahowald, N.M., Rivera Rivera, G.D., Luo, C., 2004. Comment on "Relative importance of climate and landuse in determining present and future global soil dust emission" by I. Tegen et al. Geophys. Res. Lett. 31, L24105. http://dx.doi.org/10.1029/2004GL021272.

Marshall, J.K., 1971. Drag measurements in roughness arrays of varying density and distribution. Agric. Meteorol. 8, 269–292.

Marticorena, B., Bergametti, G., 1995. Modeling the atmospheric dust cycle: 1. Design of a soil derived dust production scheme. J. Geophys. Res. 100, 16,415–16,430. http://dx.doi.org/10.1029/95JD00690.

Marticorena, B., Bergametti, G., Gillette, D.A., Belnap, J., 1997. Factors controlling threshold friction velocity in semiarid and arid areas of the United States. J. Geophys. Res. 102, 23,277–23,287. http://dx.doi.org/10.1029/97JD01303.

Marticorena, B., Chatenet, B., Rajot, J.L., Traoré, S., Coulibaly, M., Diallo, A., Koné, I., Maman, A., NDiaye, T., Zakou, A., 2010. Temporal variability of mineral dust concentrations over West Africa: analyses of a pluriannual monitoring from the AMMA Sahelian Dust Transect. Atmos. Chem. Phys. 10, 8899–8915.

Mougin, E., Lo Seen, D., Rambal, S., Gaston, A., Hiernaux, P., 1995. A regional Sahelian grassland model to be coupled with multispectral satellite data. I: model description and validation. Remote Sens. Environ. 52, 181–193. http://dx.doi.org/10.1016/0034-4257(94)00126-8.

Nickling, W.G., Gillies, J.A., 1989. Emission of fine-grained particulars from desert soils. In: Leinen, M., Sarathein, M. (Eds.), Paleometeorology: Modern and Past Patterns of Global Atmospheric Transport. Kluwer Academic, Norwell, Mass, pp. 133–165.

Nikuradse, J., 1933. Laws of flow in rough pipes (1950 translation). Tech. Rep. Technical Memorandum N°1292. National Advisory Committee on Aeronautics, Washington, DC.

Okin, G.S., Gillette, D.A., Herrick, J.E., 2006. Multi-scale controls on and consequences of aeolian processes in landscapes change in arid and semi-arid environments. J. Arid Environ. 65, 253–275. http://dx.doi.org/10.106/j.jaridenv.2005.06.029.

Pierre, C., Mougin, E., Marticorena, B., Bergametti, G., Bouet, C., Schmechtig, C., 2012. Impact of vegetation and soil moisture seasonal dynamics on dust emissions over the Sahelian belt in West Africa. J. Geophys. Res. http://dx.doi.org/10.1029/2011JD016950.

Priesley, C.H.B., 1959. Turbulent transfer in the lower atmosphere. Univ. of Chicago Press, Chicago, Ill (130 pp.).
Rajot, J.L., 2001. Windblown sediment mass budget of Sahelian village land units in Niger. Bull. Soc. Geol. Fr. 172, 523–531. http://dx.doi.org/10.2113/172.5.523.
Raupach, M.R., 1992. Drag and drag partition on rough surfaces. Bound. Layer Meteorol. 60, 375–395.
Raupach, M.R., Gillette, D.A., Leys, J.F., 1993. The effect of roughness elements on wind erosion threshold. J. Geophys. Res. 98, 3023–3029. http://dx.doi.org/10.1029/92JD01922.
Sabre, M., 1997. Etude dynamique du processus d'émission de poussières désertiques: impact sur le fractionnement physico-chimique entre sol et aérosol. (Thèse de doctorat de) l'Université Paris VII.
Schlichting, H., Gersten, K., 2000. Boundary Layer Theory, 8, ed. Springer-Verlag, Berlin.
Shao, Y., Raupach, M.R., Leys, J.F., 1996. A model for predicting Aeolians and drift and dust entrainment on scales from paddock to region. Aust. J. Soil Res. 34, 309–342. http://dx.doi.org/10.1071/SR9960309.
Spaan, W.P., van den Abeele, G.D., 1991. Wind born particle measurements with acoustic sensors. Soil Technol. 4, 51–63.
Sterk, G., Stein, A., 1997. Mapping windblown mass transport by modelling variability in space and time. Soil Sci. Soc. Am. 61, 232–239.
Swap, R., Garstang, M., Greco, S., 1992. Saharan dust in the Amazon Basin. Tellus 44B, 133–149.
Tegen, I., Fung, I., 1995. Contribution to the atmospheric mineral load from land surface modification. J. Geophys. Res. 100, 18,707–18,726. http://dx.doi.org/10.1029/95JD02051.
Tegen, I., Hollrig, P., Chin, M., Fung, I., Jacob, D., Penner, J., 1997. Contribution of different aerosol species to the global aerosol extinction optical thickness: estimates from model results. J. Geophys. Res. 102, 23895–23915. http://dx.doi.org/10.1029/97JD01864.
Tegen, I., Werner, M., Harrison, S.P., Kohfeld, K.E., 2004. Relative importance of climate and landuse in determining present and future global soil dust emission. Geophys. Res. Lett. 31, L05105. http://dx.doi.org/10.1029/2003GL019216.
Valentin, C., Rajot, J.-L., Mitja, D., 2004. Responses of soil crusting, runoff and erosion to fallowing in the sub-humid and semi-arid regions of West Africa. Agric. Ecosyst. Environ. 104, 287–302.
Wezel, A., Rajot, J.L., Herbrig, C., 2000. Influence of shrubs on soil characteristics and their function in Sahelian agro-ecosystems in semi-arid Niger. J. Arid Environ. 44, 383–398.
White, B.R., 1979. Soil transport by winds on Mars. J. Geophys. Res. 84, 4643–4651. http://dx.doi.org/10.1029/JB084iB09p04643.
Wolfe, S.A., 1993. Sparse vegetation as a surface control on wind erosion. (PhD) Univ. Guelph (257 pp.).
Yoshioka, M., Mahowald, N., Dufresne, J.-L., Luo, C., 2005. Simulation of absorbing aerosol indices for African dust. J. Geophys. Res. 110, D18S17. http://dx.doi.org/10.1029/2004JD005276.